Journal of Neurochemistry
Lippincott Williams & Wilkins, Inc., Philadelphia
© 1999 International Society for Neurochemistry

Activation of Nuclear Calcium Dynamics by Synaptic Stimulation in Cultured Cortical Neurons

*Hiroyuki Nakazawa and *†Timothy H. Murphy

*Kinsmen Laboratory, Departments of *Psychiatry and †Physiology, University of British Columbia, Vancouver, British Columbia, Canada*

Abstract: L-type voltage-sensitive Ca^{2+} channels (VSCCs) are enriched on the neuronal soma and trigger gene expression during synaptic activity. To understand better how these channels regulate somatic and nuclear Ca^{2+} dynamics, we have investigated Ca^{2+} influx through L-type VSCCs following synaptic stimulation, using the long-wavelength Ca^{2+} indicator fluo-3 combined with laser scanning confocal microscopy. Single synaptic stimuli resulted in rapid Ca^{2+} transients in somatic cytoplasmic compartments (<5 ms rise time). Nuclear Ca^{2+} elevations lagged behind cytoplasmic levels by ~60 ms, consistent with a dependence on diffusion from a cytoplasmic source. Pharmacological experiments indicated that L-type VSCCs mediated ~50% of the nuclear and somatic (cytoplasmic) Ca^{2+} elevation in response to strong synaptic stimulation. In contrast, relatively weak excitatory postsynaptic potentials (EPSPs; ~15 mV) or single action potentials were much less effective at activating L-type VSCCs. Antagonist experiments indicated that activation of the NMDA-type glutamate receptor leads to a long-lasting somatic depolarization necessary to activate L-type VSCCs effectively during synaptic stimuli. Simulation of action potential and somatic EPSP depolarization using voltage-clamp pulses indicated that nuclear Ca^{2+} transients mediated by L-type VSCCs were produced by sustained depolarization positive to −25 mV. In the absence of synaptic stimulation, action potential stimulation alone led to elevations in nuclear Ca^{2+} mediated by predominantly non-L-type VSCCs. Our results suggest that action potentials, in combination with long-lived synaptic depolarizations, facilitate the activation of L-type VSCCs. This activity elevates somatic Ca^{2+} levels that spread to the nucleus. **Key Words:** L-type voltage-sensitive calcium channels—Immediate early gene—NMDA—Imaging—Nucleus—Fluo-3.
J. Neurochem. **73,** 1075–1083 (1999).

Intracellular Ca^{2+} controls a diverse range of cell functions, including protein phosphorylation and gene expression. An unresolved issue is how normal synaptic activity is discriminated from activity that leads to gene expression. Previous studies suggest an important role for L-type voltage-sensitive Ca^{2+} channels (VSCCs) and NMDA receptors in activating immediate early genes (Murphy et al., 1991; Rosen et al., 1995; Deisseroth et al., 1996; Imprey et al., 1996; Bito et al., 1997; Ginty, 1997). We have tested the hypothesis that large sustained synaptic depolarizations lead to activation of L-type VSCCs, resulting in a rise in nuclear and cytoplasmic $[Ca^{2+}]_i$. Discrimination between normal synaptic activity and that linked to plasticity or gene expression might occur at the L-type VSCC, because single action potentials and small excitatory postsynaptic potentials (EPSPs) would be expected to largely elevate somatic Ca^{2+} levels by non-L-type VSCCs. To address these hypotheses further, we have investigated how L-type VSCCs and NMDA receptors affect Ca^{2+} dynamics in the neuronal somatic cytoplasm and nucleus. In this study, intracellular Ca^{2+} concentration $[Ca^{2+}]_i$ was monitored by using laser scanning confocal microscopy with the long-wavelength Ca^{2+} indicator fluo-3 (Minta et al., 1989). Pharmacological experiments combined with voltage-clamp pulses were used to define the stimulus requirements for activation of L-type VSCCs and for nuclear and cytoplasmic $[Ca^{2+}]_i$ elevation in response to synaptic stimulation.

EXPERIMENTAL PROCEDURES

Cell culture

Embryonic cortical neurons and glial cells (from day 18 rat fetuses) were grown 3–4 weeks in vitro on polylysine-coated glass coverslips before use in imaging experiments (as per Murphy and Baraban, 1990). Neurons and glia were plated at ~1.5×10^6 cells/ml in a 10% fetal calf serum- and 5% horse serum-containing minimal essential medium supplemented to 300 μM cystine. Cultures were fed 3 days after plating and as needed with a minimal essential medium containing 5% horse serum.

Received April 15, 1999; revised manuscript received May 13, 1999; accepted May 14, 1999.

Address correspondence and reprint requests to Dr. T. H. Murphy at Kinsmen Laboratory of Neurological Research, 4N1-2255 Wesbrook Mall, Vancouver, BC V6T 1Z3, Canada.

Abbreviations used: AM, acetoxymethyl ester; DL-APV, DL-2-amino-5-phosphonovaleric acid; CNQX, 6-cyano-7-nitroquinoxaline-2,3-dione; DMSO, dimethyl sulfoxide; EPSP, excitatory postsynaptic potential; TTX, tetrodotoxin; VSCC, voltage-sensitive Ca^{2+} channel.

Confocal imaging

Confocal imaging with a Bio-Rad MRC 600 system attached to a Zeiss upright (Axioskop) microscope was used for all experiments. Two objectives were used, either 0.9 N.A. Zeiss 63× water immersion or 0.9 N.A. Olympus 60× water immersion. The laser intensity was attenuated to 1% and the confocal pinhole was set to 3.5 (Bio-Rad units). Images were acquired using the linescan mode (3.9 ms/line) in which a 1-pixel line across the soma and nucleus is scanned repeatedly. For imaging of $[Ca^{2+}]_i$, neurons were loaded with 11 μM fluo-3 acetoxymethyl ester (AM) (Minta et al., 1989) for 50 min, or with the membrane-impermeable K^+ salt of fluo-3 by whole-cell recording (see below). To determine the position of the neuronal nucleus, images were also taken by scanning in both *x* and *y* dimensions. The nucleus was readily identifiable, because it accumulated more fluo-3 Ca^{2+} probe than the cytoplasm, consistent with the findings of O'Malley (1994). To confirm that this method of identifying the nucleus was reliable, double-labeling experiments were performed using fluo-3 (50 μM) and propidium iodide (200 μg/ml) loaded through the whole-cell patch pipette. These double-label experiments clearly indicated that the intensity of the baseline fluo-3 fluorescence could be used to identify the nuclear compartment (see Results and Fig. 1). Using *x*/*y* scanning, the approximate center of the nucleus was identified and linescan images were taken across the cytoplasm and nucleus. To synchronize delivery of field pulses with confocal image acquisition, a TTL signal from the confocal was used to trigger a second computer running pCLAMP software to produce synaptic stimuli. Confocal images were exported as byte arrays by removal of data headers and analyzed using routines written in IDL programming language (Research Systems Inc., Boulder, CO, U.S.A.) on a Pentium computer. Linescan data were analyzed by breaking the cytoplasmic and nuclear compartments of the cell into discrete regions by averaging the value of five adjacent pixels (1.1 μm). Offline averaging was done using floating point arrays to obtain additional precision over byte data (256 levels). Multiple 1.1-μm regions corresponding to cytoplasm and nucleus were averaged to improve the signal-to-noise ratio. The means of these adjacent pixels were plotted over time, and the Ca^{2+} transient amplitude was determined by integrating the transient over its rising phase (an integration time of 130 ms was used for both nuclear and cytoplasmic data).

In all of our experiments, we have reported Ca^{2+} levels as raw fluo-3 fluorescence. Experiments performed on vehicle-treated neurons indicated best stability of Ca^{2+} transients (over time) if Ca^{2+} transients were quantified in this way (see Fig. 4). We did this because in initial whole-cell perfusion experiments in which we divided changes in fluo-3 fluorescence by baseline values (dF/F_0), analysis of dimethyl sulfoxide (DMSO) vehicle control data indicated a progressive small rise in resting Ca^{2+} levels (and a decrease in dF/F_0) over the course of a whole-cell recording (average 34 ± 4%, n = 20 neurons). This small progressive rise in $[Ca^{2+}]_i$ had a large effect on the dF/F_0 ratio (attenuation over time) because resting *F* was near background levels, causing the ratio to fluctuate widely with small changes in $[Ca^{2+}]_i$. The small progressive change in baseline F_0 was associated with the length of the recording and not solvent treatment (0.1% DMSO), as neurons not treated with solvent or antagonists showed this phenomenon. We also established that there was no significant correlation between the degree of Ca^{2+} transient block by PN200-110 and baseline variation ($r = -0.0057$; data from eight neurons). Fluo-3 AM experiments showed stable resting $[Ca^{2+}]_i$ (fluo-3 fluorescence) over time; however, in this case we were unable to always measure baseline fluorescence values reliably. In these cases, baseline fluorescence levels were at times indistinguishable from background noise. Therefore, control experiments indicated that for fluo-3 AM- and fluo-3 K^+ salt-loaded neurons, the best stability of recordings (over time) was achieved when values were expressed as raw fluorescence and not a dF/F_0 ratio.

Electrophysiology

Whole-cell current clamp experiments (Hamill et al., 1981) were conducted using an Axon Instruments Axopatch 200B amplifier with 6–9 MΩ electrodes pulled from 1.5-mm glass capillaries (Warner Instruments). The patch electrodes were filled with a solution containing the following (in m*M*): 0.05 fluo-3 K^+ salt, 122 potassium methyl sulfoxide, 20 NaCl, 5 Mg-ATP, 0.3 GTP, and 10 HEPES (pH 7.2). The bath solution (continuously perfused) contained the following (in m*M*): 137 NaCl, 5.0 KCl, 2.5 $CaCl_2$, 1 $MgSO_4$, 0.34 $Na_2HPO_4 \cdot 7H_2O$, 10 NaHEPES buffer, 1 $NaHCO_3$, and 22 glucose (pH 7.4 and ~315 mosmol). Synaptic activity was blocked during voltage step and action potential (without EPSP) stimulation using a cocktail of glutamate receptor blockers, 3 μM 6-cyano-7-nitroquinoxaline-2,3-dione (CNQX) and 60 μM DL-2-amino-5-phosphonovaleric acid (DL-APV), that were obtained from Precision Biochemicals (Vancouver, BC, Canada). Membrane potentials were not corrected for an expected liquid junction potential of ~12 mV (Neher, 1995), and are likely more negative than measured. Action potentials were produced by field stimulation or under current clamp by injection of positive current. Tetrodotoxin (TTX; 0.3 μM) was added to the perfusion media to block Na^+ currents and improve clamp control in voltage-clamp experiments. Poorly voltage-clamped experiments (cells showing slow Ca^{2+} current spiking) were discarded. All solutions of PN200-110 (obtained as a gift from the Sandoz, East Hanover, NJ, U.S.A.) and Bay K-8644 (Triggle and Janis, 1987) were made fresh from frozen DMSO stocks (final DMSO concentration = 0.1%) that had been stored in the dark at −20°C.

Synaptic stimuli were delivered using pCLAMP 5 or 6 software and constant current stimulation using platinum bath electrodes (1-ms duration) (Ryan and Smith, 1995). The intensity (stimulus current) of field stimulation was adjusted over a 5–90-mA range to produce EPSPs of varying amplitude (see Results). To reduce excessive stimulation of a neuron of interest, the stimulus amplitude was set to ~50% above threshold. In some cases in which we examined the effect of single action potentials and EPSPs on Ca^{2+} dynamics mediated by L-type VSCCs (see Figs. 2B and 5) small adjustments of stimulus intensity were made to prevent multiple action potentials or action potential failure across stimulus trials. TTX (15 n*M*) was added to bath solutions in synaptic field stimulation experiments to reduce polysynaptic activity (Fields et al., 1991). Experiments performed in 20 n*M* TTX indicate that axonal excitation occurs in a reliable manner (Mackenzie and Murphy, 1998). Current clamp recordings indicated that maximal amplitude stimulation of neurons by field pulses resulted in EPSPs that were ~30 mV. In some neurons, it was possible to use relatively lower amplitude stimuli to produce graded responses of lower amplitude (see Fig. 5). To reduce the contribution of residual polysynaptic responses, Ca^{2+} transients were quantified over an initial apparently monosynaptic period (130 ms following the EPSP peak). In the case of voltage steps, responses were quantified over a 210–340-ms period following the onset of stimulation. The use of a later period for response quantification (320–450 ms) did not lead to a significant dif-

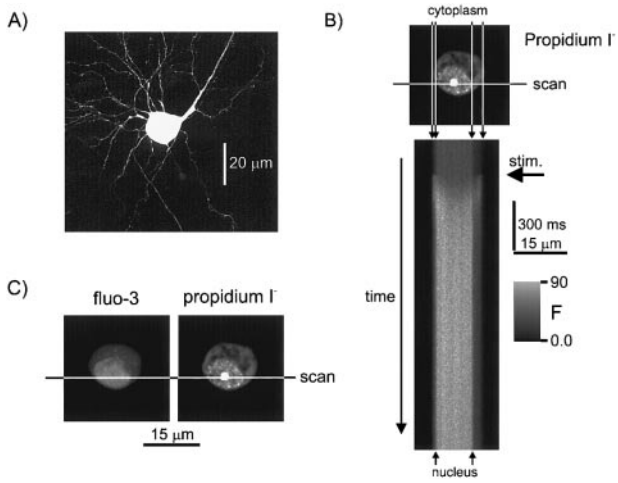

FIG. 1. Confocal imaging of the $[Ca^{2+}]_i$ indicator fluo-3 to visualize the somatic and nuclear Ca^{2+} transients after synaptic stimulation. **A:** Confocal image of live cortical neuron loaded with fluo-3 by whole-cell recording. **B:** Confocal optical section of propidium iodide fluorescence over the same area indicating localization of the nucleus (elevated signal). The vertical lines indicate putative compartmentalization of the nucleus from the cytoplasm. The **lower panel** shows an image of 480 confocal linescans oriented with zero time at the top of the image (fluo-3 data). The *x* dimension of this figure corresponds to distance across the neuronal cytoplasm and nucleus. Regions corresponding to the nuclear boundary are indicated by arrows. The *y* dimension is time, with each linescan in this image taking 3.9 ms. The position of the linescan image (over time) through the somatic area is indicated in C. Arrow (stim.) denotes the time of synaptic stimulation. Scale bar indicates fluo-3 fluorescence in units of pixel value. **C:** Single optical section at the level of nucleus showing colocalization of fluo-3 basal fluorescence and propidium iodide staining.

ference in the fraction of the nuclear Ca^{2+} transient that was blocked by PN200-110.

RESULTS

Ca^{2+} dynamics in somatic and nuclear compartments in response to depolarization and synaptic stimuli

We have used the Ca^{2+} indicator fluo-3 (both its K^+ salt and AM forms) to evaluate the kinetics and pharmacology of the nuclear and cytoplasmic (somatic) $[Ca^{2+}]_i$ transient that was evoked by synaptic stimulation (field stimulation), action potentials, and voltage steps. For our experiments, we have chosen spiny cortical neurons in culture, which resemble large pyramidal neurons. A fluo-3 image showing the shape of a typical neuron is shown in Fig. 1A. The nucleus was readily visible in optical sections as it accumulates more fluo-3 dye than the cytoplasm (Fig. 1B and C), consistent with the findings of O'Malley (1994). Double-labeling experiments with propidium iodide, a nucleic acid stain (Arndt-Jovin and Jovin, 1989), confirmed that fluo-3 accumulation can be used to identify the nucleus. To improve the time resolution of Ca^{2+} imaging, we used the linescan mode of confocal microscopy (Fig. 1B, lower panel; 3.9 ms/line). In the linescan mode, a 1-pixel line is scanned consecutively 480 times through the neuronal cytoplasm and nucleus within a 1-μm optical section. An image of the linescan data was created by stacking consecutive scans in order of time (Fig. 1B, lower panel). Examination of the linescan image reveals a "smile-like" pattern at the onset of stimulation (voltage step used), in which Ca^{2+}-induced fluorescence changes are first detected within the cytoplasm and then later within the nucleus.

Stimulation of cortical neurons with field stimulation induced synaptic activity (an EPSP with usually one action potential; see Experimental Procedures) and resulted in a rapid rise in cytoplasmic Ca^{2+} levels in the neuronal soma (Fig. 2A). After a short delay (~60 ms), $[Ca^{2+}]_i$ was elevated within nuclear compartments. Analysis of EPSPs indicated that these local rises in nuclear and cytoplasmic $[Ca^{2+}]_i$ were associated with depolarizations that were sufficient to trigger action potentials. $[Ca^{2+}]_i$ rose more slowly in the nucleus than in the cytoplasm (Fig. 2A). Detailed analysis of the re-

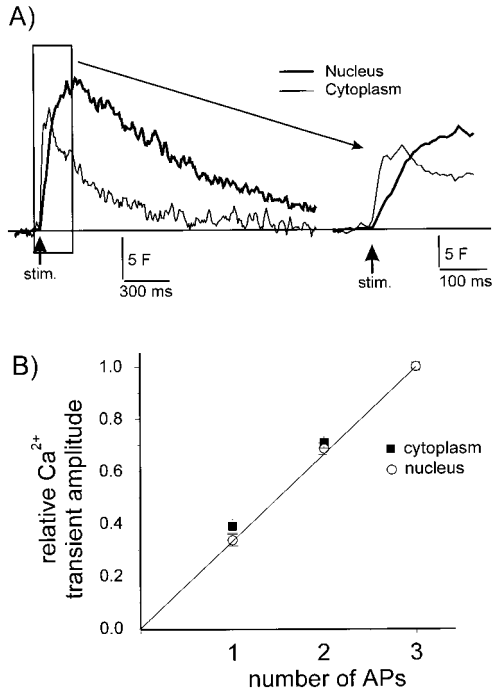

FIG. 2. Kinetics and linearity of the nuclear $[Ca^{2+}]_i$ transient in response to synaptic stimulation. **A:** Shown are plots of fluo-3 fluorescence for both cytoplasmic and nuclear regions of a neuron synaptically stimulated with a single field pulse. To improve the signal-to-noise ratio, all regions of the neuronal cytoplasm and the nucleus were averaged from the linescan data (as in Fig. 1). On the **right** side of the figure, a higher-resolution plot of nuclear and cytoplasmic Ca^{2+} dynamics is shown. F indicates units of pixel value. **B:** Example of Ca^{2+} transient linearity in response to one, two, or three action potentials (APs) elicited by field stimulation in DL-APV and CNQX (200-ms interval between stimuli). The plot was constructed from data obtained from n = 9 fluo-3 AM-loaded neurons. The error bars depict the SEM. Responses were normalized to the amplitude observed with three action potentials for each compartment (nucleus and cytoplasm). The line indicates perfect linearity.

TABLE 1. *Pharmacological analysis of synaptic Ca^{2+} transients in fluo-3 AM-loaded cells*

	n	Nucleus	Cytoplasm
% of control Ca^{2+} transient			
Control		100	100
Bay K-8644 (1 μM)	5	216 ± 32[a]	229 ± 68[a]
DL-APV (80 μM)	13	70 ± 9[d]	62 ± 5[c]
PN200-110 (1 μM)	22	54 ± 3[d]	59 ± 4[d]
PN200-110 + DL-APV	29	50 ± 4[d]	48 ± 4[d]
% of each antagonist			
Control (DL-APV)		100	100
PN200-110 + DL-APV/DL-APV	13	69 ± 7[d]	64 ± 5[d]
Control (PN200-110)		100	100
PN200-110 + DL-APV/PN200-110	16	88 ± 4[b]	88 ± 8[a]

Values are means ± SEM of n fluo-3-loaded neurons stimulated by field pulses and represent the % of the control Ca^{2+} transient recorded in the absence of the indicated antagonists. The units of the control Ca^{2+} transient are pixel value as described in Experimental Procedures. The % control Ca^{2+} transient was calculated by dividing the baseline-subtracted change in fluo-3 fluorescence observed in the presence of antagonists (F_{ant}) by that observed in their absence (F_{con}); % control $[Ca^{2+}]_i$ transient = $(F_{ant}/F_{con}) * 100$. In the lower half of the table, changes in the $[Ca^{2+}]_i$ transient were evaluated under conditions in which 80 μM DL-APV and 1 μM PN200-110 were used as controls. Paired *t* tests were performed to assess statistical significance.

[a] $p < 0.05$; [b] $p < 0.01$; [c] $p < 0.005$; [d] $p < 0.001$.

sponse to a single action potential indicated that cytoplasmic Ca^{2+} levels were elevated to 63% of maximum within 4.4 ± 0.7 ms, whereas nuclear levels required 58 ± 5 ms to reach the same level (n = 17).

Signal linearity can be problematic when using relatively high-affinity Ca^{2+}-sensitive probes such as fluo-3 (Minta et al., 1989) to study changes in $[Ca^{2+}]_i$. To address this, we produced varying numbers of action potential-inducing field stimuli (CNQX and DL-APV present, no EPSP observed) and checked the relationship between the rise in nuclear and cytoplasmic fluo-3 fluorescence as a function of the number of stimuli. These data fit well to a line (one to three stimuli given, n = 9 cells) for both the nucleus and the cytoplasm, suggesting that under our conditions the fluo-3 fluorescence response (raw pixel change) is proportional to the degree of stimulation (Fig. 2B).

L-type VSCCs mediate a component of the nuclear Ca^{2+} transient

To isolate the specific class of ion channels that trigger the rise in nuclear $[Ca^{2+}]_i$, pharmacological experiments were conducted on fluo-3 AM-loaded neurons with specific antagonists (PN200-110) and agonists (Bay K-8644) for L-type VSCCs (Table 1; Triggle and Janis, 1987). Parallel experiments performed in neurons that were not loaded with fluo-3 indicated that the field stimulus parameters used resulted in large EPSPs (~30 mV) with one or more action potentials. The use of PN200-110 (1 μM) indicated that L-type VSCCs mediate ~50% of the Ca^{2+} transient in both the nucleus and the somatic cytoplasm. No significant difference in the contribution of L-type VSCCs in nuclear versus cytoplasmic Ca^{2+} influx was observed (Table 1).

In contrast to the effects of the L-type VSCC antagonist, Bay K-8644 (1 μM), an L-type Ca^{2+} VSCC agonist, produced a doubling of both nuclear and cytoplasmic Ca^{2+} elevation in response to field synaptic stimulation (Table 1). Although the L-type VSCC agonist increased the peak level of Ca^{2+} reached, it did not affect the rise time for the nuclear Ca^{2+} transient (data not shown). The rise time of the nuclear Ca^{2+} transient was examined, because we thought by analogy to results from muscle tissue that the nuclear Ca^{2+} transient may have a regenerative component facilitated by Ca^{2+}-induced Ca^{2+} release (Cheng et al., 1996; Rio and Stern, 1997). We also compared the rise time of the nuclear Ca^{2+} transient in the presence of an L-type VSCC antagonist to control conditions and observed no difference. For example, with a 130-ms step depolarization to −15 mV (a stimulus in which ~50% of the Ca^{2+} transient is mediated by L-type VSCCs; Fig. 3A), the rise time (63% of maximum) of the nuclear $[Ca^{2+}]_i$ transient for the control and PN200-110-treated neurons was 113.9 ± 6.2 and 111.0 ± 6.0 ms, respectively (n = 9).

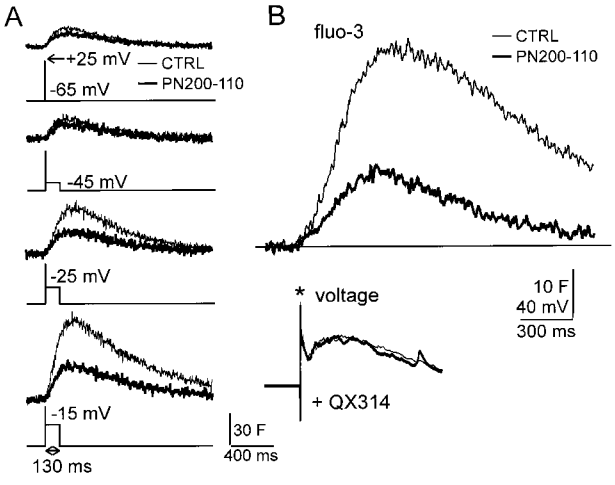

FIG. 3. Effect of simulated and actual EPSPs on nuclear and cytoplasmic Ca^{2+} dynamics. **A:** In voltage-clamp mode, a large fast depolarization (−65 to +25 mV for 3 ms) and then various degrees of steady depolarizations (−65 to −15 mV for 130 ms) were delivered to characterize the requirements for activation of L-type VSCCs. Higher levels of steady depolarization resulted in an enhanced Ca^{2+} transient that was PN200-110-sensitive (thick trace). Data from a single neuron representative of 10 are shown. **B:** Large long-lasting EPSPs activate L-type VSCCs [average record of nuclear and cytoplasmic Ca^{2+} dynamics (three trials) from linescan imaging]. Ca^{2+} transients mediated by large EPSPs (>30 mV) were reduced significantly by PN200-110 (1 μM) [average record (three trials) of membrane potential obtained under whole-cell current clamp mode for the cell shown above]. A large EPSP (>40 mV) without an action potential is shown. The initial fast component of the voltage record is associated with the field stimulus artifact. Resting membrane potentials of these neurons averaged −53 ± 2 mV (n = 8). Internal application of the Na^+-channel blocker QX-314 was used to block multiple Na^+ action potentials that result from large EPSPs.

TABLE 2. *Effects of Ca^{2+}-channel blockers on the Ca^{2+} transient mediated by a single action potential*

% of control Ca^{2+} transient	n	Cytoplasm	Nucleus
Control	21	100	100
PN200-110 (1 μM)	21	80.6 ± 5.2	79.2 ± 4.2
p		<0.001	<0.001
Control	5	100	100
Toxins	5	55.9 ± 13.4	44.6 ± 9.5
p		<0.05	<0.005

Combined application of ω-agatoxin IVA (200 n*M*), ω-conotoxin GVIA (1 μM), and ω-conotoxin MVIIC (1 μM), which block P-, N-, and Q-type Ca^{2+} channels, respectively, attenuated the nuclear and cytoplasmic Ca^{2+} transient stimulated by a single action potential by ~50%, whereas PN200-110 had little effect. All responses are normalized to the control response without drugs. Action potentials were elicited by field stimulation of fluo-3 AM-loaded neurons in the presence of DL-APV and CNQX. Values are means ± SEM; paired *t* tests were performed to assess statistical significance. See Table 1 for explanation of % control Ca^{2+} transient calculation.

The role of NMDA receptors in facilitating nuclear Ca^{2+} transients

Analysis of fluo-3 AM-loaded neurons indicated that the addition of the NMDA receptor antagonist DL-APV (50 μM) resulted in a significant attenuation of both nuclear and cytoplasmic Ca^{2+} dynamics (~30% reduction for the nucleus) in response to synaptic stimuli (Table 1). It is interesting that when DL-APV was applied to neurons pretreated with the L-type Ca^{2+}-channel blocker PN200-110, a smaller attenuation of nuclear or cytoplasmic $[Ca^{2+}]_i$ was observed (Table 1). This result suggests that NMDA receptors facilitate L-type VSCC activity (presumably by depolarization), leading to Ca^{2+} entry into somatic compartments. NMDA receptor antagonists also reduced the amplitude of a slow, apparently polysynaptic, EPSP (see Fig. 3B for example of slow EPSP). To measure more accurately the slow EPSP, we calculated the average change in membrane potential for a 130-ms period after presynaptic stimulation in the presence and absence of DL-APV. Addition of DL-APV reduced the slow EPSP from 31.6 ± 1.0 mV to 7.9 ± 2.4 mV ($p < 0.005$, n = 4 cells), suggesting a mechanism for reduction in L-type VSCC activation.

Ca^{2+} dynamics in response to action potential stimulation

Pharmacological experiments on the Ca^{2+} response to a single action potential (performed in fluo-3 AM-loaded neurons in DL-APV and CNQX) indicated that both nuclear and cytoplasmic Ca^{2+} dynamics were weakly blocked by L-type VSCC blockers (~20% reduction; see Table 2). Current clamp recording indicated that under the conditions used (DL-APV and CNQX included) EPSPs were blocked and that field stimulation results in the generation of a single action potential (Prange and Murphy, 1999). Under these conditions, the ~50% of the Ca^{2+} transient could be blocked by a cocktail of P-, N-, and Q-type Ca^{2+}-channel peptide antagonists (see Table 2). It is possible that the action potential-evoked Ca^{2+} transient remaining after the toxin treatment is mediated by T-type Ca^{2+} channels (Ertel and Ertel, 1997). To determine the relative role of action potential firing versus subthreshold depolarization in eliciting nuclear and somatic cytoplasmic Ca^{2+} elevations, we induced action potentials in neurons with current injection in the presence of blockers of excitatory synaptic transmission (DL-APV/CNQX). Rapid elevations in cytoplasmic and subsequent nuclear $[Ca^{2+}]_i$ were observed in response to a single action potential elicited by brief current injection (2–5 ms, 0.2–0.5 nA, n = 12 neurons; data not shown). An action potential was required, as subthreshold stimulation failed to result in a significant cytoplasmic or nuclear Ca^{2+} transient (n = 9 neurons; data not shown).

Simulated action potentials and EPSPs indicate a role for L-type Ca^{2+} channels during long-lasting strong EPSPs

In experiments performed in synaptically stimulated fluo-3 AM-loaded neurons, we observed a significant reduction in the amplitude of both nuclear and cytoplasmic $[Ca^{2+}]_i$ transients (elicited by synaptic stimulation) in the presence of PN200-110 (Table 1). In these experiments, field stimulus intensity was generally set to levels that were 50% greater than response threshold. One limitation of this method was that without parallel electrophysiological recordings, we did not know to what degree these stimuli affected membrane potential. To understand better the requirements for synaptic activation of L-type VSCCs, voltage-clamp pulses were delivered to simulate the effects of action potentials and EPSPs on $[Ca^{2+}]_i$ dynamics (Fig. 3A). Using a 3-ms pulse to +25 mV (action potential-like stimulation) and varying degrees of steady EPSP-like depolarization (0–50 mV, for 130 ms) from −65 mV holding potential, the role of L-type VSCCs was examined by PN200-110 treatment. In control experiments (without PN200-110), relatively small changes in $[Ca^{2+}]_i$ were observed with the 3-ms action potential-like step (Fig. 3). The addition of steady EPSP-like depolarization resulted in a significant increase in the amplitude of both the nuclear and cytoplasmic Ca^{2+} transient (one-way analysis of variance, n = 10 neurons, $p < 0.0001$; Figs. 3A and 4A). Analysis of group data with PN200-110 treatment indicated that L-type VSCCs were activated significantly only during relatively strong depolarizations positive to −25 mV (one-way analysis of variance, n = 10 neurons, with the Newman–Keuls multiple comparison test, $p < 0.01$; Fig. 4A). In contrast to the effect of PN200-110, in separate experiments DMSO vehicle (0.1%) had no significant effect on the amplitude of the nuclear Ca^{2+} transient (Fig. 4B). To examine the relative effect of transient action potential firing versus steady depolarization on Ca^{2+} transients, we compared simulated EPSPs with and without a superimposed action potential waveform. We observed that the presence of an action potential had little effect on the $[Ca^{2+}]_i$ transient evoked by sustained depolarization to potentials positive to −35

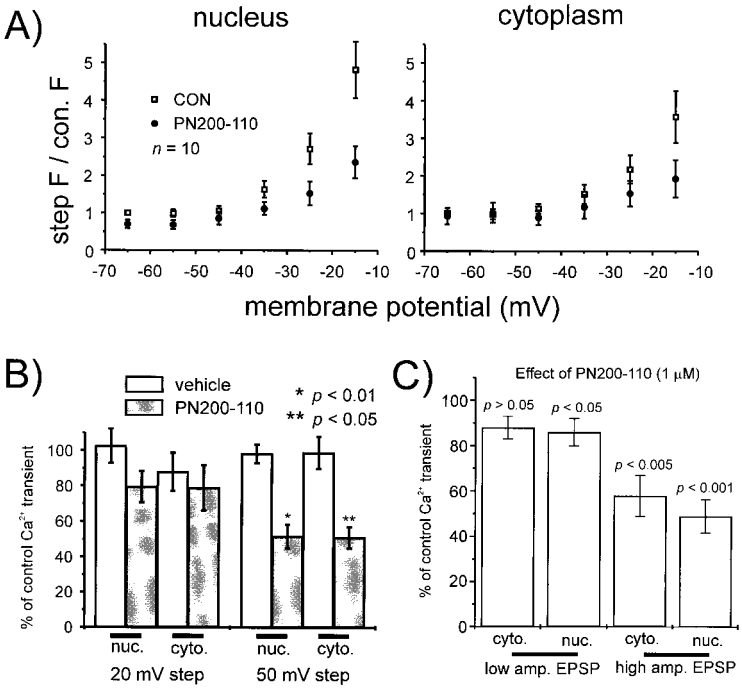

FIG. 4. Strong depolarization is necessary to activate L-type VSCCs. **A:** Group data for simulated EPSPs and spikes as in Fig. 3A. All responses are normalized to a control response mediated by initial large action potential-like step (3 ms, −65 to +25 mV) in the absence of PN200-110. An effect of PN200-110 is observed with steady depolarization to potentials positive to −35 mV. Values are means ± SEM of n = 10 cells. **B:** The effects of PN200-110 (1 μM; n = 10 neurons) and DMSO vehicle (0.1%; n = 9 neurons) are compared in paradigms that depolarize by 20 and 50 mV for 130 ms. With 50 mV of steady depolarization, a significant effect of PN200-110 was observed (paired *t* test). All trials were preceded by a 3-ms action potential-like step to +25 mV (as in Fig. 3A). **C:** Effect of PN200-110 on Ca^{2+} transients mediated by large and small EPSPs (group data). All responses are normalized to the control responses in the absence of PN200-110 (1 μM). Values are means ± SEM; n = 8 for cells with low-amplitude EPSPs (16.9 ± 2.6 mV for control and 17.7 ± 2.7 mV for PN200-110) and n = 8 for cells with high-amplitude EPSPs (32.9 ± 1.7 mV for control and 33.0 ± 2.4 mV for PN200-110). Paired *t* tests were performed to assess the significance of potential differences between groups.

mV. For example, steady depolarization (130 ms) to −25 mV produced a Ca^{2+} transient in the nucleus that did not change amplitude significantly in the absence of an action potential. The Ca^{2+} transient produced by steady depolarization to −25 mV was 96.2 ± 5.9% (nucleus) and 100.9 ± 7.9% (cytoplasm) of that observed with a steady depolarization plus an action potential-like step ($p > 0.1$, n = 9). Although pharmacological experiments suggested a clear role for L-type channels during strong depolarization, the effect of PN200-110 was not complete, indicating a possible role for other high-threshold and noninactivating VSCC types. It is interesting that the non–PN200-110-sensitive component was likely not mediated by P-, N-, and Q-type Ca^{2+} channels as the combined application of ω-agatoxin IVA (200 nM), ω-conotoxin GVIA (1 μM), and ω-conotoxin MVIIC (1 μM), respectively, did not reduce significantly the nuclear Ca^{2+} transient associated with an action potential-like depolarization followed by 130 ms of EPSP-like depolarization to −15 mV under voltage clamp (responses were 93 ± 17% of control values, n = 7 neurons).

Large synaptically evoked EPSPs effectively activate L-type Ca^{2+} channels

Experiments using the voltage-step paradigm (Fig. 3A) indicated that steady depolarization to potentials positive to −25 mV were most effective at activating L-type VSCCs. Therefore, we examined whether similarly sized EPSPs in the absence of action potentials might also activate these channels (Fig. 3B). To produce large EPSPs, the field stimulus intensity was increased until EPSP amplitudes were ~30 mV or greater. These large stimuli usually resulted in the recruitment of a slower polysynaptic EPSP (Fig. 3B). To prevent the contamination of the signals by action potentials (which have little role in $[Ca^{2+}]_i$ transients with sustained depolarization; see above), the Na^+-channel blocker QX-314 (Connors and Prince, 1982) was included in the recording pipette. Under these conditions, large EPSPs reliably resulted in a nuclear Ca^{2+} transient in which L-type VSCCs made a significant contribution, as the addition of PN200-110 reduced this Ca^{2+} response by 51.1 ± 7.4% (n = 8, $p < 0.001$). In a separate group of QX-314-treated neurons, DMSO vehicle did not produce any effect on the nuclear Ca^{2+} transient (Ca^{2+} transient observed in DMSO vehicle was 106.2 ± 5.0% of that observed in control solutions; n = 10, $p > 0.1$). Comparison of group data for large and small EPSPs indicated a significantly greater role of L-type VSCCs with the large EPSPs (Fig. 4C). Analysis of group data also indicated that PN200-110 treatment did not significantly reduce the EPSP amplitude under the conditions we used (Fig. 4 legend). In contrast to the effects of the large-amplitude EPSPs and voltage steps, Ca^{2+} transients mediated by relatively small ~15-mV EPSPs and a single action potential were largely insensitive to PN200-110 (1 μM; Fig. 5). Similar results were observed in a total of eight neurons (nuclear and cytoplasmic Ca^{2+} transients were 86 ± 6 and 88 ± 5% of control values, respectively, in the presence of 1 μM PN200-110).

DISCUSSION

Immunocytochemical evidence indicates that L-type VSCCs are enriched on the neuronal soma (Westenbroek et al., 1990, 1992). Due to the sensitivity of activity-dependent gene expression to antagonists of L-type VSCCs and the strategic location of the channels on the

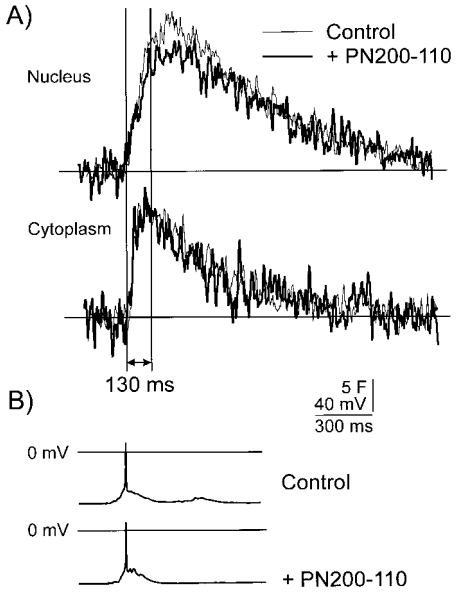

FIG. 5. L-type VSCC blockers have little effect on the synaptic $[Ca^{2+}]_i$ transient in both the cytoplasm and nucleus induced by small EPSPs (~15 mV) that lead to one action potential. **A:** Record of nuclear and cytoplasmic Ca^{2+} dynamics obtained from linescan imaging. Addition of PN200-110 (thick trace) has little effect on the Ca^{2+} transient evoked by the small EPSP and a spike. An average of three trials of stimulation from a single cell are shown. **B:** Average record of membrane potential (three trials) obtained under whole-cell current clamp mode for the cell shown above (A) in the presence or absence of PN200-110 (1 μM). Neither the small EPSP (~15 mV) nor the spike was affected by PN200-110. Resting membrane potentials of these neurons averaged -66 ± 2 mV (n = 8).

neuronal soma, L-type VSCCs have been proposed to play a critical role in Ca^{2+}-dependent gene expression (Murphy et al., 1991; Bading et al., 1993; Deisseroth et al., 1996, 1998; Bito et al., 1997). It is interesting that most reports show a relatively small role for the L-type VSCC in mediating Ca^{2+} influx in response to synaptic or action potential stimuli. For example, Regehr and Tank (1992) and Christie et al. (1995) demonstrated that ~30% of the Ca^{2+} transient evoked by a train of action potentials was attributed to L-type VSCCs. Recent findings by Deisseroth et al. (1998) indicate that L-type VSCCs are critical for activity-dependent cyclic AMP response element binding protein phosphorylation, but that P/Q-type VSCCs have a more significant role in $[Ca^{2+}]_i$ elevation in response to KCl. In this study, we have examined more carefully the stimulus requirements for activation of L-type VSCCs in pyramidal type cultured cortical neurons.

Pharmacological analysis of Ca^{2+} dynamics in response to synaptic stimulation

Using relatively strong synaptic field stimulation, we observed that the addition of an L-type VSCC blocker suppressed the Ca^{2+} transient in both the nucleus and the cytoplasm. Parallel membrane potential measurements showed that this degree of synaptic stimulation resulted in large EPSPs (~30 mV) and action potentials. The requirement for large long-lasting EPSPs is consistent with the biophysical properties (Nowycky et al., 1985; Tsien et al., 1988) of L-type VSCCs. These slow EPSPs were reduced by the addition of the NMDA receptor antagonist DL-APV. In cells pretreated with DL-APV, the effect of an L-type VSCC antagonist was reduced (Table 1). The reduced effect of an L-type VSCC antagonist (in the presence of DL-APV) suggested that NMDA receptors might produce the long-lasting depolarization required to activate this channel type, explaining why both NMDA receptor antagonists and L-type VSCC blockers can attenuate activity-dependent gene expression (Murphy et al., 1991; Deisseroth et al., 1996, 1998; Imprey et al., 1996; Liu and Graybiel, 1996). In other systems, for example, hippocampal dentate gyrus long-term potentiation-induced gene expression, effects of NMDA receptor antagonists may be attributed to secondary blockade of L-type VSCC activation (Cole et al., 1989). In our system, we do not believe that the effects of NMDA antagonists are mediated directly by attenuating direct NMDA receptor-mediated Ca^{2+} influx into the soma, as excitatory synapses are localized to dendrites and diffusion of Ca^{2+} from a dendritic source would be too slow (Murphy et al., 1995) to account for the rapid rise in cytoplasmic Ca^{2+} observed.

Measurement of nuclear and cytoplasmic Ca^{2+} dynamics

By examining the time lag versus the distance traveled from the cell membrane to the center of the nucleus, we established that the elevation in nuclear Ca^{2+} associated with synaptic stimulation was consistent with a diffusional mechanism, although we cannot exclude a role for amplification by Ca^{2+} release from intracellular stores. A recent preliminary modeling study by J. Ren and T. H. Murphy (to be presented at the 29th Meeting of the Society for Neuroscience, 1999) suggests that Ca^{2+} stores greatly facilitate Ca^{2+} elevations in nuclear compartments in response to L-type VSCC activation. Prolonged changes in nuclear Ca^{2+} levels that are attributed to Ca^{2+} stores have been reported previously in hippocampal neurons challenged with glutamate (Korkotian and Segal, 1996). With regard to a diffusional mechanism, we observed an average latency between nuclear and cytoplasmic Ca^{2+} dynamics of ~60 ms. Using published values for cytoplasmic Ca^{2+} diffusion [233 $\mu m^2/s$ (Allbritton et al., 1992; Kasai and Petersen, 1994)], we determined that the delay (between cytoplasmic and nuclear Ca^{2+} elevation) was consistent with a dependence on a diffusional mechanism as observed in studies performed in other cell types [mast cell tumor lines (Allbritton et al., 1994), bullfrog sympathetic neurons (Hernández-Cruz et al., 1990), and *Xenopus laevis* oocytes (O'Malley, 1994)]. The distance to the nucleus from the plasma membrane is ~5 μm; given a diffusion constant of 233 $\mu m^2/s$, a diffusion-mediated process would take ~100 ms to reach that point (Kasai and Petersen, 1994). The estimate of diffusion time is within twofold of our

observed value. In examining the kinetics of the Ca^{2+} transient decay, we noticed that the nuclear Ca^{2+} transient decayed considerably slower than that in the cytoplasm. Although this result seems to suggest a prolonged Ca^{2+} transient in the nucleus, it could also arise from a higher fluo-3 concentration and increased buffering (Tank et al., 1995) within nuclear compartments. Furthermore, we have observed that nuclear fluorescence signals were of larger absolute amplitude than those measured in the cytoplasm. Previous studies indicated that fluo-3 signals are significantly enhanced (in amplitude) in nuclear compartments even with clamped saturating $[Ca^{2+}]_i$ levels (O'Malley, 1994; Perez-Terzic et al., 1997). Because of this potential error, we have restricted our analysis to relative changes in $[Ca^{2+}]_i$ levels between the nucleus and cytoplasm and have not made absolute comparisons of amplitude.

Selective activation of L-type VSCCs during large excitatory postsynaptic potentials

Small EPSPs and action potentials produced a Ca^{2+} transient in the neuronal soma that was only marginally sensitive to L-type VSCC antagonists. Action potential-evoked Ca^{2+} transients were significantly more sensitive to blockers of P/Q- and N-type channels than those that block L-type VSCCs. The result that L-type VSCCs are only weakly activated by action potentials is surprising given that P/Q-, N-, and L-type channels have similar activation voltages (Bourinet et al., 1996). Mermelstein et al. (1998) propose that the relatively low sensitivity of action potential-evoked Ca^{2+} influx to L-type VSCC blockers is due to the channel's relatively slow activation kinetics. They also propose that preferential activation of L-type VSCCs during EPSP-like voltage steps is due to a more negative activation potential for L-type VSCCs.

Although L-type VSCCs are activated by large EPSPs, antagonists of this channel only reduce the Ca^{2+} transient by ~50%. The reason for incomplete block of the Ca^{2+} transient by PN200-110 could be attributed to several factors: first, the presence of Ca^{2+}-channel types (non-L, N, and P/Q) that are insensitive to PN200-110, or an incomplete block by PN200-110. It is possible that higher concentrations of PN200-110 would produce a complete block of the nuclear Ca^{2+} transients; however, experiments with 3 μM PN200-110 failed to result in a higher degree of block (data not shown). The literature suggests that 1 μM PN200-110 should be sufficient to block completely the L-type VSCC under hyperpolarized conditions (Triggle and Janis, 1987).

A model for nuclear Ca^{2+} elevation

Many models of synaptic modulation indicate that plastic stimuli, i.e., those that might trigger gene expression, are inherently different from normal synaptic transmission. For example, high-frequency trains of activity are required to produce long-term potentiation, whereas low-frequency stimulation results in depression (Linden and Connor, 1995). Our findings suggest that L-type VSCCs are activated by strong sustained depolarization. We propose that stimulus paradigms that result in synchronized activation of multiple neuronal inputs might bring neurons to these depolarized potentials. Although this is likely to result in multiple action potentials, this effect would allow sufficient activation of L-type VSCCs. Such stimuli might occur during the high-frequency trains that are used to produce late forms of long-term potentiation that are dependent on gene expression (Bolshakov et al., 1997). Although intense sustained depolarization is required to activate L-type VSCCs, their action can be facilitated by agents that increase intracellular cyclic AMP (Dolphin, 1996). In this manner, effects of dopamine and forskolin that enhance late long-term potentiation (Bailey et al., 1996) could be attributed to a facilitation of L-type VSCC activity. In addition, neuromodulators such as serotonin and norepinephrine could act by affecting intracellular cyclic AMP levels and a modulation of the L-type VSCC (Braha et al., 1993). By facilitating L-type VSCC activity, neuromodulators may enable low-amplitude EPSPs and trains of stimuli to elevate $[Ca^{2+}]_i$ without resulting in a large degree of burst-type activity.

Acknowledgment: We would like to thank Dr. S. Wang and Dr. Dee Brink of the University of British Columbia for helpful comments on the manuscript. This work was supported by grants from the Medical Research Council of Canada, the EJLB Foundation, and NARSAD (Young Investigator Award to T.H.M.). T.H.M. is a Medical Research Council of Canada scientist.

REFERENCES

Allbritton N. L., Meyer T., and Stryer L. (1992) Range of messenger action of calcium ion and inositol 1,4,5-triphosphate. *Science* **258,** 1812–1815.

Allbritton N. L., Oancea E., Kuhn M. A., and Meyer T. (1994) Source of nuclear calcium signals. *Proc. Natl. Acad. Sci. USA* **91,** 12458–12462.

Arndt-Jovin D. J. and Jovin T. M. (1989) Fluorescence labeling and microscopy of DNA. *Methods Cell Biol.* **30,** 417–448.

Bading H., Ginty D. D., and Greenberg M. E. (1993) Regulation of gene expression in hippocampal neurons by distinct calcium signaling pathways. *Science* **260,** 181–186.

Bailey C. H., Bartsch D., and Kandel E. R. (1996) Toward a molecular definition of long-term memory storage. *Proc. Natl. Acad. Sci. USA* **93,** 13445–13452.

Bito H., Deisseroth K., and Tsien R. W. (1996) CREB phosphorylation and dephosphorylation: a Ca^{2+}- and stimulus duration-dependent switch for hippocampal gene expression. *Cell* **87,** 1203–1214.

Bito H., Deisseroth K., and Tsien R. W. (1997) Ca^{2+}-dependent regulation in neuronal gene expression. *Curr. Opin. Neurobiol.* **7,** 419–429.

Bolshakov V. Y., Golan H., Kandel E. R., and Siegelbaum S. A. (1997) Recruitment of new sites of synaptic transmission during the cAMP-dependent late phase of LTP at CA3–CA1 synapses in the hippocampus. *Neuron* **19,** 635–651.

Bourinet E., Zamponi G. W., Stea A., Soong T. W., Lewis B. A., Jones L. P., Yue D. T., and Snutch T. P. (1996) The α_{1E} calcium channel exhibits permeation properties similar to low-voltage activated calcium channels. *J. Neurosci.* **16,** 4983–4993.

Braha O., Edmonds B., Sacktor T., Kandel E. R., and Klein M. (1993) The contributions of protein kinase A and protein kinase C to the actions of 5-HT on the L-type Ca^{2+} current of the sensory neurons in *Aplysia. J. Neurosci.* **13,** 1839–1851.

Cheng H., Lederer M. R., Xiao R. P., Gomez A. M., Zhou Y. Y., Ziman B., Spurgeon H., Lakatta E. G., and Lederer W. J. (1996) Excitation–contraction coupling in heart: new insights from Ca^{2+} sparks. *Cell Calcium* **20,** 129–140.

Christie B. R., Eliot L. S., Ito K., Miyakawa H., and Johnston D. (1995) Different Ca^{2+} channels in soma and dendrites of hippocampal pyramidal neurons mediate spike-induced Ca^{2+} influx. *J. Neurophysiol.* **73,** 2553–2557.

Cole A. J., Saffen D. W., Baraban J. M., and Worley P. F. (1989) Rapid increase of an immediate early gene messenger RNA in hippocampal neurons by synaptic NMDA receptor activation. *Nature* **340,** 474–476.

Connors B. W. and Prince D. A. (1982) Effects of local anesthetic QX-314 on the membrane properties of hippocampal pyramidal neurons. *J. Pharmacol. Exp. Ther.* **220,** 476–481.

Deisseroth K., Bito H., and Tsien R. W. (1996) Signaling from synapse to nucleus: postsynaptic CREB phosphorylation during multiple forms of hippocampal synaptic plasticity. *Neuron* **16,** 89–101.

Deisseroth K., Heist E. K., and Tsien R. W. (1998) Translocation of calmodulin to the nucleus supports CREB phosphorylation in hippocampal neurons. *Nature* **392,** 198–202.

Dolphin A. C. (1996) Facilitation of Ca^{2+} current in excitable cells. *Trends Neurosci.* **19,** 35–43.

Ertel S. I. and Ertel E. A. (1997) Low-voltage-activated T-type Ca^{2+} channels. *Trends Pharmacol. Sci.* **18,** 37–42.

Fields R. D., Yu C., and Nelson P. G. (1991) Calcium, network activity, and the role of NMDA channels in synaptic plasticity. *J. Neurosci.* **11,** 134–146.

Ginty D. D. (1997) Calcium regulation of gene expression: isn't that spatial? *Neuron* **18,** 183–186.

Hamill O. P., Marty A., Neher E., Sakmann B., and Sigworth F. (1981) Improved patch-clamp techniques for high resolution current recordings from cells and cell free membrane patches. *Pflügers Arch.* **391,** 85–100.

Hernández-Cruz A., Sala F., and Adams P. R. (1990) Subcellular calcium transients visualized by confocal microscopy in a voltage-clamped vertebrate neuron. *Science* **247,** 858–862.

Imprey S., Mark M., Villacres E. C., Poser S., Chavkin C., and Storm D. R. (1996) Induction of CRE-mediated gene expression by stimuli that generate long-lasting LTP in area CA1 of the hippocampus. *Neuron* **16,** 973–982.

Kasai H. and Petersen O. H. (1994) Spatial dynamics of second messengers: IP_3 and cAMP as long-range and associative messengers. *Trends Neurosci.* **17,** 95–101.

Korkotian E. and Segal M. (1996) Lasting effects of glutamate on nuclear calcium concentration in cultured rat hippocampal neurons: regulation by calcium stores. *J. Physiol. (Lond.)* **496,** 39–48.

Linden D. J. and Connor J. A. (1995) Long term synaptic depression. *Annu. Rev. Neurosci.* **18,** 319–357.

Liu F.-C. and Graybiel A. M. (1996) Spatiotemporal dynamics of CREB phosphorylation: transient versus sustained phosphorylation in the developing striatum. *Neuron* **17,** 1133–1144.

Mackenzie P. J. and Murphy T. M. (1998) High safety factor for action potential conduction along axons but not dendrites of cultured hippocampal and cortical neurons. *J. Neurophysiol.* **80,** 2089–2101.

Mermelstein P. G., Pitt G. S., Bito H., Deisseroth K., and Tsien R. W. (1998) L-type calcium channels support a selective response of nuclear CREB phosphorylation to EPSPs rather than action potentials. *Soc. Neurosci. Abstr.* **24,** 7.

Minta A., Kao J., and Tsien R. Y. (1989) Fluorescent indicators for cytosolic calcium based on rhodamine and fluorescein chromophores. *J. Biol. Chem.* **264,** 8171–8178.

Murphy T. H. and Baraban J. M. (1990) Glutamate toxicity in immature cortical neurons precedes development of glutamate receptor currents. *Dev. Brain Res.* **57,** 146–150.

Murphy T. H., Worley P. F., and Baraban J. M. (1991) L-type voltage-sensitive calcium channels mediate synaptic activation of immediate early genes. *Neuron* **7,** 625–635.

Murphy T. H., Baraban J. M., and Wier W. G. (1995) Mapping miniature synaptic currents to single synapses using calcium imaging reveals heterogeneity in postsynaptic output. *Neuron* **15,** 159–168.

Neher E. (1995) Voltage offsets in patch-clamp experiments, in *Single-Channel Recording* (Sakmann B. and Neher E., eds), pp. 147–153. Plenum Press, New York.

Nowycky M. C., Fox A. P., and Tsien R. W. (1985) Three types of neuronal calcium channels with different calcium agonist sensitivity. *Nature* **316,** 440–443.

O'Malley D. O. (1994) Calcium permeability of the neuronal nuclear envelope: evaluation using confocal volumes and intracellular perfusion. *J. Neurosci.* **14,** 5741–5758.

Perez-Terzic C., Stehno-Bittel L., and Clapham D. E. (1997) Nucleoplasmic and cytoplasmic differences in the fluorescence of the calcium indicator fluo-3. *Cell Calcium* **21,** 275–282.

Prange O. and Murphy T. M. (1999) Analysis of multiquantal transmitter release from single cultured cortical neuron terminals. *J. Neurophysiol.* **81,** 1810–1817.

Regehr W. G. and Atluri P. P. (1995) Calcium transients in cerebellar granule cell presynaptic terminals. *Biophys. J.* **68,** 2156–2170.

Regehr W. G. and Tank D. W. (1992) Calcium concentration dynamics produced by synaptic activation of CA1 hippocampal pyramidal cells. *J. Neurosci.* **12,** 4202–4223.

Rio E. and Stern M. D. (1997) Calcium in close quarters: microdomain feedback in excitation–contraction coupling and other cell biological phenomena. *Annu. Rev. Biophys. Biomol. Struct.* **26,** 47–82.

Rosen L. B., Ginty D. D., and Greenberg M. E. (1995) Calcium regulation of gene expression. *Adv. Second Messenger Phosphoprotein Res.* **30,** 225–253.

Ryan T. and Smith S. J. (1995) Vesicle pool mobilization during action potential firing at hippocampal synapses. *Neuron* **14,** 983–989.

Tank D. W., Regehr W. G., and Delaney K. R. (1995) A quantitative analysis of presynaptic calcium dynamics that contribute to short-term enhancement. *J. Neurosci.* **15,** 7940–7952.

Triggle D. J. and Janis R. A. (1987) Calcium channel ligands. *Annu. Rev. Pharmacol. Toxicol.* **27,** 347–369.

Tsien R. W., Lipscombe D., Madison D. V., Bley K. R., and Fox A. P. (1988) Multiple types of neuronal calcium channels and their selective modulation. *Trends Neurosci.* **11,** 431–438.

Westenbroek R. E., Ahlijanian M. K., Madison D. V., Bley K. R., and Fox A. P. (1990) Clustering of L-type Ca^{2+} channels at the base of major dendrites in hippocampal pyramidal neurons. *Nature* **347,** 281–284.

Westenbroek R. E., Hell J. W., Warner C., Dubel S. J., Snutch T. P., and Catterall W. A. (1992) Biochemical properties and subcellular distribution of an N-type calcium channel alpha 1 subunit. *Neuron* **9,** 1099–1115.